Revisiting the role of 3-nitrotyrosine residues in the formation of alpha-synuclein oligomers and fibrils

Cecilia Chavarría[1,2]*, Rodrigo Ivagnes[1,2]*, Ari Zeida[1,2], María Dolores Piñeyro[1],[3], José M. Souza[1,2]

[1]Departamento de Bioquímica, [2]Centro de Investigaciones Biomédicas (CEINBIO), Facultad de Medicina, Universidad de la República, Av. Gral. Flores 2125, Montevideo 11800, Uruguay.
[3]Laboratorio de Interacciones Hospedero-Patógeno, Unidad de Biología Molecular, Institut Pasteur de Montevideo, Mataojo 2020, Montevideo 11400, Uruguay.

*Both authors contributed equally

Abbreviations: α-synuclein (a-syn); Parkinson's disease (PD); Thioflavin T (Th-T); peroxynitrite ($ONOO^-$); nitric oxide ($^{\bullet}NO$); superoxide anion ($O_2^{\bullet-}$); hydroxyl radical ($OH^{\bullet}$); hydrogen peroxide (H_2O_2); nitrogen dioxide radical ($^{\bullet}NO_2$); carbonate radical ($CO_3^{\bullet-}$); circular dichroism (CD); hydrodynamic radius (RH); transmission electron microscopy (TEM); dynamic light scattering (DLS).

Correspondence should be addressed to José M. Souza. Mail to: jsouza@fmed.edu.uy

Highlights

- Nitration of tyrosine residues within a-syn hinders the formation of fibrils.
- The presence of a single 3-nitrotyrosine residue, situated at either the N- or C-terminal of a-syn, prevents a-syn fibrillization.
- Tyrosine nitration doesn´t impede oligomer formation in a-syn.
- Tyrosine nitration might promote the generation of off-pathway oligomers, potentially amplifying neurotoxicity.

Abstract

Nitration of tyrosine residues in alpha-synuclein (a-syn) has been detected in different synucleinopathies, including Parkinson´s disease. The potential role of 3-nitrotyrosine formation in a-syn, as an oxidative post-translational modification, is still elusive. In this work, we generated well-characterized tyrosine nitrated a-syn monomers and studied their capability to form oligomers and fibrils. We constructed tyrosine to phenylalanine mutants, containing a single tyrosine residue, a-syn mutant Y(125/133/136)F and Y(39/125/133)F) and assessed the impact in a-syn biophysical properties. Nitrated wild-type a-syn and the Y-F mutants, with one 3-nitrotyrosine residue in either the protein's N-terminal or C-terminal region, showed inhibition of fibril formation but retained the capacity of oligomer formation. The inhibition of a-syn fibrillation occurs even when an important amount of unmodified a-syn is still present. We characterized oligomers from both nitrated and non-nitrated forms of the wild-type protein and the mutant forms obtained. Our results indicate that the formation of 3-nitrotyrosine in a-syn could induce an off-pathway oligomer formation which may have an important impact in the development of synucleinopathies.

Keywords: alpha-synuclein, post-translational modification, 3-nitrotyrosine, fibrils, oligomers.

Graphical Abstract

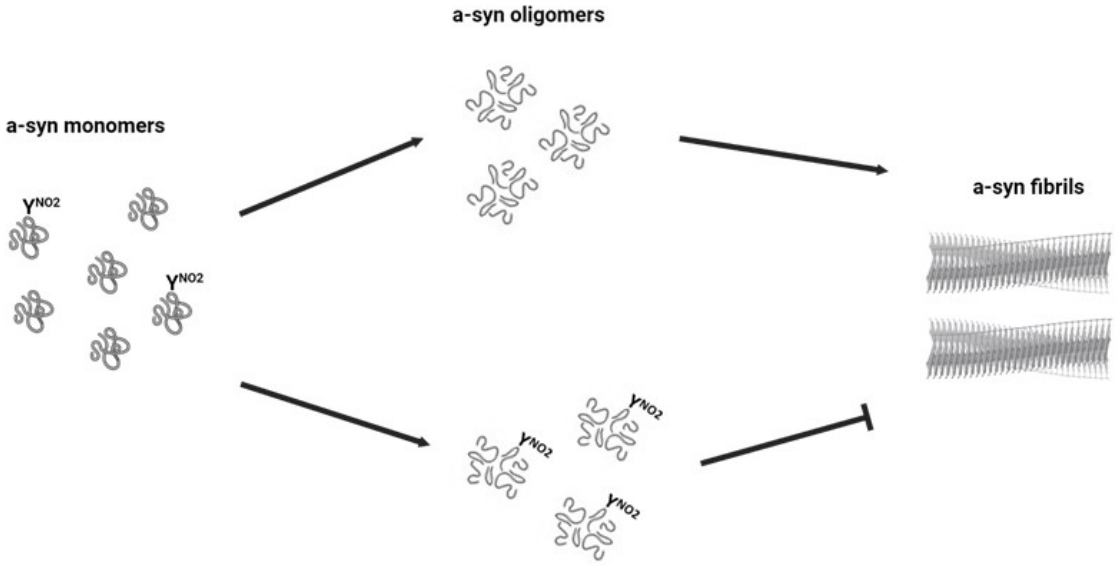

Introduction

Alpha-synuclein (a-syn) is a small cytoplasmic protein of 140 amino acids, which is expressed in many regions of the brain and in red blood cells [1,2]. The protein belongs to the group of intrinsically disordered proteins, with no defined structure in solution [3]. It is well established that the aggregation of a-syn is a key pathological feature of several neurodegenerative diseases, including Parkinson's disease (PD) and dementia with Lewy bodies (DLB), which are collectively known as alpha-synucleinopathies [4]. The accumulation of a-syn aggregates in Lewy bodies, proteinaceous inclusions that develop inside neurons or in non-neuronal cells during neurodegeneration, is a hallmark of these diseases [5–7].

The link between a-syn and disease has been established through genetic evidence and histopathological observations. Missense mutations in the a-syn gene (*SNCA*) lead to the accumulation of a-syn, neuroinflammation, and degeneration of the striatal neurons [8]. Immunohistochemical detection of a-syn in tissue samples from Lewy bodies of PD and DLB patients has provided compelling evidence for the role of a-syn in these diseases [9].

Fibril formation is a key event in the process of a-syn aggregation. It follows a nucleation-dependent process, in which monomeric a-syn forms oligomers of different sizes and morphologies. Some oligomeric species do not continue down the nucleation pathway and remain in an "off-pathway" state, which does not proceed to fibril formation [10]. Others grow through the addition of monomers and form mature fibrils with characteristic beta-sheet structures. Understanding the mechanisms underlying a-syn aggregation is crucial for developing effective therapies for alpha-synucleinopathies. Many factors influence a-syn fibril propensity, such as specific cellular conditions (changes in pH, temperature, ionic strength), macromolecular crowding, and interaction with other ligands (amyloidogenic proteins, metal ions, intermediary toxic species, membranes, and specific lipid molecules)[11,12].

In pathological conditions, including neurodegenerative diseases, the increase in intracellular oxidative stress can generate reactive oxygen and nitrogen species,

including peroxynitrite ($ONOO^-$), nitric oxide ($^{\bullet}NO$), superoxide anion ($O_2^{\bullet-}$), hydroxyl radical ($OH^{\bullet}$), hydrogen peroxide (H_2O_2), nitrogen dioxide radical ($^{\bullet}NO_2$), and carbonate radical ($CO_3^{\bullet-}$), among others. $ONOO^-$ does not react directly with tyrosine but generates one-electron oxidants that can oxidize tyrosine to tyrosyl radical ($Tyr^{\bullet}$), and the nitrogen dioxide radical ($^{\bullet}NO_2$), which react in a radicalar manner, leading to the formation of 3-nitrotyrosine residues in proteins [13]. Oxidative damage to a-syn can alter its ability to form fibrils, bind to membranes, and be degraded by the proteasome [14,15]. For a-syn, methionine oxidation, 3-nitrotyrosine formation, and di-tyrosine crosslink have been identified as hallmarks of oxidative stress [16–19].

Histopathological evidence of the role of a-syn nitration in pathology came from the detection of nitrated a-syn in brain tissue from post-mortem PD patients using immunostaining techniques [20]. The detection of nitrated a-syn in sera and peripheral blood mononuclear cells of patients with PD also supports the biomedical relevance of oxidative post-translational modifications [21]. Although the mechanism by which oxidation and nitration of a-syn affects the fibrillation process is not yet fully defined, many investigators have shown that a-syn nitration and oxidation completely inhibit fibril formation [18,19,22]. Burai et al. demonstrated that different nitrated a-syn species exhibit distinct structural and aggregation properties using site-specific tyrosine nitration and chemical ligation [23].

To elucidate the effect of 3-nitrotyrosine formation on a-syn, we constructed tyrosine to phenylalanine mutants and characterized them using various techniques. We examined the impact of post-translational oxidative modifications on a-syn oligomer and fibril formation, and analyzed whether the 3-nitrotyrosine residue position in the protein could influence the oligomerization and/or fibrilization process.

Materials and Methods

Primer design

The primers were designed according to the manufacturer's instructions using the software Primer Blast (NCBI) and the Oligo Analyzer TM Tool (Integrated DNA Technologies). Primer synthesis was performed under standard conditions (Integrated DNA Technologies) and primers were used at a final concentration of 100 ng/µl. Primer sequences are listed in Supplementary Table 1.

Generation of the a-syn mutant constructs

Site-directed mutagenesis using QuikChange II Site-Directed Mutagenesis kit (Agilent Technologies, SC, USA) was performed following the manufacturer's instructions. Two synthetic oligonucleotide primers with the desired mutation, each complementary to one vector strand were designed and used to generate the mutated plasmid by PCR amplification. The reaction was performed in the pET-30 plasmid containing human a-syn gene construct as a template (DNA template used 50-100 ng), using the Pfu turbo DNA polymerase (Invitrogen), with 100 ng/µl of sense and antisense primers for each mutant, dNTPs and reaction buffer. Amplification conditions were as follows: initial denaturing at 95°C for 2 minutes and 25 cycles of 30 seconds at 95°C, 30 seconds using each primer annealing temperature (Tm) - 5°C, a 6-minute elongation step at 72°C, and a final 10-minute extension at 72°C. Following temperature cycling, the DNA containing the desired mutation was selected by treating the PCR product with restriction enzyme DpnI (0.2U/µL), which degrades methylated parental DNA. All the mutations were confirmed by sequencing.

Protein expression and purification

Wild-type and mutant a-syn were expressed in *Escherichia coli* BL21 (DE3) as a recombinant protein and purified as described previously [3]. The purification was

confirmed using SDS-PAGE 12% and the pure protein was diluted in 10 mM Tris pH 7.4 and stored at -80°C.

Protein quantification

Protein concentration was determined spectrophotometrically at 280 nm using ε_{280nm} of 5600 $M^{-1}cm^{-1}$ for a-syn wild-type and ε_{280nm} of 1490 $M^{-1}cm^{-1}$ for a-syn Y-F mutants, calculated using the ProtParam tool from Expasy https://web.expasy.org/protparam/). Alternatively, protein concentrations were determined using the bicinchoninic acid protein (BCA) assay (Sigma) using bovine serum albumin as a standard.

Exposure of a-syn to peroxynitrite and DNI

Peroxynitrite was synthesized from the reaction between sodium nitrite ($NaNO_2$) and acidified H_2O_2 as described previously [24]. The concentration of peroxynitrite was determined spectrophotometrically at 302 nm in 0.1 M NaOH (ε_{302nm} is 1700 $M^{-1}cm^{-1}$). Protein (1.43 mg/ml) was dissolved in nitration buffer (100 mM sodium phosphate, 25 mM sodium bicarbonate, and 0.1 mM diethylenetriaminepentaacetic acid, pH 7.4), in the presence of 5 mM $NaNO_2$. Peroxynitrite was added in two doses to achieve a final concentration of 0.5 mM. A relation of 1:5 protein/nitrating agent was used. The reagent 5-methyl-1,4-dinitro-1H-imidazole (DNI) was used as an alternative method to nitrate tyrosine residues in a-syn, as previously described [25,26]. a-Syn (0.7 mg/ml) was incubated in 25 mM sodium phosphate buffer pH 6.0 with DNI (1 mM) and irradiated with UV-A light for 30 min.

Mass spectrometry

An ESI-triple quadrupole mass spectrometer (QTrap4500, ABSciex) was employed for detection. The spectrometer was set in Q1 positive mode in the 500-1500 m/z range with a scan rate of 200 Da/s and Q1 resolution in UNIT. The parameters used were as follows: IS, 5000; TEM, 300; DP, 120; EP, 10; CUR, 20; GS1, 30; GS2, 20. Data acquisition was done using Analyst 1.6.2 (ABSciex) and PeakView

2.2 (ABSciex) software was used for data analysis and deconvolution of all spectra. ESI-MS was performed on protein samples before and after the reaction with $ONOO^-$ to identify the oxidative modification detected.

Fibrillation assays

Wild-type or mutant a-syn (100 µM) was incubated at 37°C in the nitration buffer with agitation at 1400 rpm in Thermomixer (Eppendorf®). Fibril formation was followed by an increase in Thioflovine T (Th-T) fluorescence. Aliquots were taken at different time points and mixed with 10 µM Th-T in 50 mM Glycine-NaOH pH 8.5. Fluorescence emission spectra were recorded from 465–600 nm with excitation at 450 nm and an emission wavelength of 482 nm was plotted against time. Th-T fluorescence measurements were performed on a JASCO 8500 spectrofluorimeter using a 10 mm light path quartz cuvette.

Aliquots of 10 µL of a-syn fibril samples (as described above) taken at different time points were diluted in 140 µL of Congo red solution (20 µM Congo red 20 mM Tris pH 7.5, 100 mM NaCl) in a 96 well clear plate with flat bottom. The plate was left at room temperature for 15 minutes and absorbance at 540 nm and 480 nm was measured in a plate reader (Varioskan Flash). Results were analyzed as the ratio between 540nm/480nm absorbance.

Oligomer preparation

We selected the method proposed by Apetri *et al*. to prepare a-syn oligomers [27]. Briefly, freeze-dried monomeric a-syn (4.28 mg/ml) was incubated in 10 mM Hepes buffer pH 7.4 at 37°C without stirring. After 20 h of incubation, the oligomers were separated and purified from the monomeric protein through filtration, using an Amicon 100 kDa cut-off filter.

To obtain nitrated oligomers, protein samples (1.43 mg/ml) were previously exposed to $ONOO^-$ (0.5 mM), freeze-dried, and then we followed the same procedure described before to purify oligomers.

Circular dichroism

The circular dichroism (CD) spectra of wild-type a-syn and mutant (0.1 mg/ml in 5 mM Tris buffer pH 7.4) forms were measured using a CD spectrometer Applied Photophysics (Chirascan V100) in the far UV region (190-260 nm) using a 0.1 cm path length cuvette. 2 mM SDS was added and changes in the CD spectra were recorded in these conditions. A total of four spectra for each condition were recorded and averaged.

Aliquots taken at the Th-T assay were measured at the CD spectrometer to follow fibril formation using this technique. For each time point, aliquots of 20 µL were taken and diluted in 20 mM phosphate buffer pH 7.4.

Dynamic light scattering

The size distribution of monomeric and oligomeric a-syn species was determined by dynamic light scattering (Zetasizer NanoS, Malvern Instruments Ltd). For each sample (0.3 mg/ml protein in 10 mM Hepes pH 7.4), the total light scattered at an angle of 90° was collected using a 10-second acquisition time. Particle translational diffusion coefficients were calculated from the autocorrelated light intensity data and converted to hydrodynamic radius (RH) using the Stokes-Einstein equation. Analysis was done using the software provided by Malvern Instruments and Raynals algorithm (https://spc.embl-hamburg.de/app/raynals) [28]. The correlation functions and fittings for selected experimental conditions can be appreciated in supplementary Figure S1.

Transmission electron microscopy

Samples were stained with 1% uranyl acetate for 2 minutes and images were obtained in a JEOL JEM-1010 transmission electron microscope using Formvar-coated carbon grids (200 mesh).

Data analysis

Experiments were performed at least three times on independent days. All data are represented as means ± SD unless otherwise stated. Means were compared using unpaired t-test, one-way or two-way ANOVA, followed by Tukey's multiple comparisons test or Sidak's multiple comparisons test. Statistical significance was considered with P-value < 0.05. All statistical analyses were performed using GraphPad Prism 8.0 software.

Results

Characterization of monomeric a-syn and a-syn mutants

a-Syn contains four tyrosine residues; Y39 located in the N-terminal region and Y125, Y133, and Y136 located in the C-terminal region (Scheme 1). To study the influence of these tyrosine residues and 3-nitrotyrosine formation on a-syn fibrillation and oligomer formation, we generated mutants on these tyrosine residues by site-directed mutagenesis. Specifically, we constructed Y(125/133/136)F and Y(39/125/133)F mutants, which have only one remaining tyrosine residue. We then characterized the a-syn monomers using dynamic light scattering (DLS) and circular dichroism (CD). The CD spectra of all forms of a-syn showed the characteristic profile of a random coil protein, with a minimum of around 200 nm, and no significant differences were observed between the wild-type protein and the mutant forms. The addition of 2 mM SDS induced the formation of α-helical structures, as evidenced by the presence of negative minima at 222 nm and 208 nm and a maximum at 190 nm, a phenomenon previously described for wild-type a-syn [29] (Figure 1A). DLS data revealed significant variations in the hydrodynamic radius among monomeric a-syn, with Y(125/133/136)F appearing smaller than WT and Y(39/125/133)F larger than its WT counterpart (Figures 1B, 1C, and S1). Despite these specific statistical differences, the overall size of monomeric a-syn remains within a comparable range.

In this work, we confirmed that the a-syn tyrosine to phenylalanine mutants showed no significant differences in the CD spectra however, discernible differences emerged in the DLS analysis when compared to the wild-type protein and between both mutants.

Effects of peroxynitrite on a-syn oligomer and fibril formation

We also investigated whether the presence or absence of tyrosine residues could affect a-syn oligomer formation. Oligomers are high molecular weight species, and this term refers to a population of aggregated a-syn that has not acquired a fibrillar conformation. We used the method developed by Apetri et al. to prepare a-syn oligomers from both wild-type protein and the Y-F mutants [27,30]. The yield of oligomer formation under these experimental conditions was 4%, and the purity was confirmed by native electrophoresis. All mutants showed the ability to form oligomers with the same yield as the wild-type protein (data not shown). These findings suggest that the presence or absence of tyrosine residues does not significantly impact a-syn oligomer formation.

According with other authors, the freeze-dry preparation method for a-syn oligomers introduces some heterogeneity in the oligomeric population [31]. Our observations revealed two distinct DLS populations of oligomers, with one species measuring between 6-12 nm and a minor population between 70-100 nm (Figures 2B and S1). Notably, the 6-12 nm oligomers constitute the predominant species, a finding consistent with TEM images (Figures 2C) and the literature [31]. The DLS data further indicate that the small-size oligomers derived from a-syn Y-F mutants Y(125/133/136)F and Y(39/125/133)F) are 1.3 and 1.7 times smaller, respectively, compared to those from wild-type a-syn (Figure 2B).

TEM data also supported these findings, showing that oligomers formed from the Y-F mutants were smaller and had a chain-like structure compared to the rounded shape of the wild-type a-syn oligomers, with diameters ranging from 28.54 - 115.3 nm (Figure 2C). These results suggest that the tyrosine residues may play a role in the compactness of the oligomers or the number of monomers per oligomer formed, as indicated by the changes observed when tyrosine residues were replaced with phenylalanine.

We investigated the impact of peroxynitrite treatment on a-syn and its Y-F mutants' ability to form oligomers. Following peroxynitrite treatment, the morphology and size of the resulting oligomers were similar to wild-type oligomers, except for the

Y(39/125/133)F which presents a smaller radius (1.3 folds smaller) and Y(125/133/136)F which has a larger radius (1.2 times) (Figure 2A and B).

We conducted a series of experiments to assess the fibril-forming ability of the Y-F mutants of a-syn and compare their morphology to wild-type a-syn fibrils. Our findings suggest that the a-syn Y-F mutants form fibrils at a similar rate to wild-type a-syn (Figure 3A). However, TEM images of fibrils revealed that the fibrils formed by the a-syn Y-F mutants are thinner than those formed by wild-type protein (Figure 3B). Additionally, we monitored fibril formation using CD spectra and obtained aliquots at various time points throughout the aggregation assay (Figure 3C). Far-UV-CD spectra indicated a transition from a random coiled spectrum to a beta-sheet structure, without an observable alpha-helix intermediate.

The formation of fibrils was impeded by pretreatment of a-syn with peroxynitrite, as evidenced by Thioflavin-T assay and CD spectra (Figure 3A, C). The inhibitory effect was observed regardless of the location of the 3-nitrotyrosine residue, as both a-syn mutants, Y(125/133/136)F and Y(39/125/133)F, displayed complete inhibition of fibril formation after peroxynitrite treatment. Notably, we discovered that the presence of only one 3-nitrotyrosine residue, either at the C-terminal or N-terminal of a-syn, was sufficient to hinder fibril formation (Figure 3A, C). These findings indicate that the nitration of a single tyrosine residue can significantly affect the protein´s ability to form fibrils, without affecting oligomer formation.

The lower pKa of the hydroxyl group in 3-nitrotyrosine, compared to tyrosine residues [32], may result in an increase in negative charges at pH 7.4, potentially hindering the interaction of monomers that can form fibrils and it may impact fibril formation. Fibril formation of wild-type a-syn exposed to $ONOO^-$ was not recovered by lowering pH (Figure 3D), acidic pH eliminates negative charges formed due to a lower pKa of 3-nitrotyrosine, suggesting that the increase in negative charge is not responsible for fibril inhibition.

Profile of post-translational oxidative modifications in a-syn wild-type and Y-F mutants

Tyrosine residues in proteins are susceptible to oxidation forming mainly 3-nitrotyrosine and di-tyrosine. As a-syn has neither cysteine nor tryptophan residues, the targets for oxidation are mainly tyrosine and methionine residues. Given that treatment of proteins with $ONOO^-$ results in a mixture of oxidized species, we analyze the profile of oxidative modifications in a-syn wild-type and Y-F mutants exposed to $ONOO^-$ by mass spectrometry, to characterize the components in aggregation assays. Purified wild-type a-syn showed the corresponding calculated mass of 14.457,5 Da and also a small amount of +16 Da that could correspond to one oxidized methionine residue, probably generated during protein purification. This was also observed in the a-syn mutants Y(125/133/136)F and Y(39/125/133)F, with the corresponding molecular weight of 14.412,1 Da and +16 Da species.

Treatment of wild-type a-syn and the Y-F mutant with $ONOO^-$ yield different numbers of tyrosine nitrated and methionine oxidized residues, as well as an important amount of the unmodified protein. Treatment of wild-type a-syn with $ONOO^-$ results in the incorporation of one nitro group (+45 Da), representing 24.7% of the total species formed, and also a 10.7% of two nitrated tyrosine residues (+ 90 Da) without a significant increase in oxidation. In the sample, there was also 35.6% of the unmodified monomeric protein and a small proportion of other species (Figure 4). However, as indicated in Figure 4, the profile of oxidative modification is quite different for wild-type a-syn than for Y-F a-syn mutants. Treatment of both Y-F mutants with $ONOO^-$, yields a higher amount of the nitrated form, which corresponds to the +45 Da increase in mass. The unmodified protein is the second species in abundance. Also, there are nitrated mutant forms with one oxidized methionine in a small proportion. Protein oxidation and nitration under our experimental conditions did not change the CD spectra observed from monomeric proteins and still formed alpha-helical structures in the presence of 2 mM SDS as seen by CD spectra (Supplementary Figure S2).

Due to the generation of some methionine sulfoxide residues in a-syn by peroxynitrite treatment, a different new method for inducing the formation of 3-

nitrotyrosine was used [25,26]. The protein was treated with 5-methyl-1,4-dinitro-1H-imidazole (DNI) and irradiated with UV-A light. DNI irradiated with UV-A light homolyzes to $^{\bullet}NO_2$ and nitroimidazole radicals, which generate 3-nitrotyrosine residue, via the formation of tyrosyl radical intermediate [25,26]. The oxidation profile was equivalent in both methods, being tyrosine nitration the main oxidative modification. However, for wild-type a-syn the yield of 3-nitrotyrosine formation was higher with DNI than with $ONOO^-$, obtaining 60% of a-syn fully nitrated (the four tyrosine residues nitrated), 10% of tri-nitrated a-syn species, without the presence of unmodified protein. The formation of methionine sulfoxide is 20%, mainly coming from protein purification. In these conditions practically there was only a small amount of methionine sulfoxide generated by DNI (Figure 5A, B). a-Syn treated with DNI showed also a complete inhibition of fibril formation, supporting the role of 3-nitrotyrosine residues in a-syn as an oxidative post-translational modification impedes the development of a-syn fibrils (Figure 5C). We generated a new a-syn mutant Y(39/125/133/136)F, which substitutes all tyrosine residues with phenylalanine to investigate the fibrillation of a-syn following treatment with $ONOO^-$ or with DNI and UV-A. Our results revealed that DNI treatment had no impact on the fibrillation of Y(39/125/133/136)F a-syn, as it does not oxidize methionine residues significantly (Figure 5C). Conversely, the absence of tyrosine residues in a-syn led to an increase in methionine sulfoxide generation upon $ONOO^-$ treatment, consequently inhibiting fibril formation (Figure 5B, C). The a-syn treated with DNI and UV-A light was still able to form oligomer species (Figure 5D), as it was shown for a-syn and Y-F mutants treated with $ONOO^-$ (Figure 2). These data confirm that 3-nitrotyrosine formation in monomeric a-syn does not affect oligomers assembly.

Discussion

The purpose of this study is to investigate the impact of oxidative modifications on the aggregation properties of a-syn, particularly tyrosine nitration, by designing and purifying a-syn tyrosine to phenylalanine mutants. It is still not clear which of these species, oligomers or fibrils, are involved in cellular toxicity and neurodegeneration, so it is relevant to determine the structural characteristics of these species. Previous studies have reported that C-terminal residues interact with N-terminal residues in a way that may promote different tridimensional structures [33]. In this work, we showed that oligomers obtained from the a-syn mutant Y(125/133/136)F and Y(39/125/133)F) are 1.3 and 1.7 smaller than the ones obtained from a-syn wild-type. In addition, they differ in shape; a-syn wild-type oligomers present rounded shape and the ones obtained from the Y-F mutant are punctiform (Figure 2). These results suggest a role of tyrosine residues in the process of oligomer formation, generating more compact oligomeric structures when tyrosine is changed by phenylalanine residue or maybe the presence of phenylalanine instead of tyrosine may generate oligomers with less monomer per unit of oligomer formed. The mutants Y-F also generate thinner fibrils than the wild-type protein (Figure 3). Both results seem consistent with the idea that phenylalanine residues allow closer contact between monomers than tyrosine residues in a-syn fibrillization process.

Under pathological conditions, such as neurodegenerative diseases, there is an increase in the levels of reactive nitrogen and oxygen species, leading to the formation of peroxynitrite among other reactive species. The exposure of proteins to peroxynitrite induces the formation of 3-nitrotyrosine, dityrosine cross-links, and methionine sulfoxides. We are interested in investigating these ‘complex’ samples because *in vivo*, the increase in the formation of oxidants in the brain could probably induce the simultaneous nitration and sulfoxidation of a-syn. Previous data showed that a-syn exposure to peroxynitrite induces the formation of nitrated a-syn and dityrosine cross link monomers that prevent the progression of a-syn to form fibrillar species [17]. Hodara *et al.* showed that nitrated dimeric a-syn can promote fibril formation, but nitrated monomeric a-syn inhibited it, consistent with

the results present here (Figure 3) [14]. Tyrosine nitration of wild-type a-syn or the mutants Y-F, with only one tyrosine present (Y(125/133/136)F or Y(39/125/133)F), induced a complete inhibition of a-syn fibril formation (Figure 3). In this way, the presence of only one 3-nitrotyrosine residue, in either the N-terminal or the C-terminal side of the protein, produces an inhibition of the fibrillation of a-syn. Mass spectrometry analysis of these nitrated a-syn species showed the formation of 3-nitrotyrosine residues and methionine sulfoxide, as well as an important amount of non-modified protein (Figure 4). The nitrated species are capable of affecting the fibrillation process of the unmodified a-syn, supporting a gain of function of the nitrated a-syn. The fibrillation of a-syn can be inhibited by 3-nitrotyrosine residues, possibly due to a decrease in the pKa of the hydroxyl group or an increase in the size of the modified residue [34]. Interestingly, the inhibitory effect of 3-nitrotyrosine residues was not alleviated at acidic pH (Figure 3), which suggests that the bulkiness of the nitro group on the modified tyrosine residue is the main factor contributing to the inhibition of fibril formation. It was shown that methionine sulfoxide residues also inhibit fibril formation of a-syn [35]. Because peroxynitrite induces a small degree of methionine oxidation in a-syn, we employed a different nitration method [25,26]. DNI irradiation with UV-A generates nitrated a-syn without oxidation of methionine residues, resulting in all tyrosine residues being nitrated (Figure 5). These findings support the significant impact of 3-nitrotyrosine residues on a-syn in fibril formation. However, the development of a-syn oligomers remains unaffected by the presence of 3-nitrotyrosine residues, whether there are multiple nitrated tyrosine residues or only one (Figures 2 and 5). In the study by Chen *et al.*[31] the oligomeric a-syn population was meticulously characterized through analytical ultracentrifugation, revealing predominantly two species 10S and 15S. We replicate the same methodology to generate oligomers, suggesting a likely resemblance in the oligomer distribution. In a prior study, we analyzed the cellular effect of oligomers from wild-type a-syn, uncovering their ability to induce mitochondrial dysfunction, ROS production and pro-inflammatory cytokine release in primary rat astrocytes [30]. Subsequent studies are required to comprehensively examine whether 3-nitrotyrosine in a-syn contributes to the enrichment of the 10S

or 15S species and delineate its biological effects. Our findings suggest that even small quantities of nitrated a-syn formed under pathological conditions can influence the aggregation process of a-syn. Oligomeric forms of a-syn have been proposed as a primary factor contributing to early neuronal toxicity [36,37]. Additionally, extracellular fibrillar a-syn exhibits prion-like behavior, implying its involvement in disease propagation within the central nervous system (CNS) [38,39]. Both a-syn species, oligomers, and fibrils, exert distinct and significant effects on neuron and glial cells [30,40,41].

The formation of 3-nitrotyrosine in a-syn is proposed to stabilize the formation of oligomeric species via an off-pathway mechanism. Simultaneously, it inhibits fibril development, potentially leading to the production of more intracellular toxic species. This post-translational modification may represent a gain of function induced by the nitration process.

Acknowledgements and Fundings

Dr. Mauricio Mastrogiovanni for Mass Spectrometry assistance. Dr. Federico Carrión for his help in the experiments performed with the Dynamic Light Scattering equipment from the Institut Pasteur Montevideo. Dr. Gabriela Casanova and Gaby Martínez, from Facultad de Ciencias, for their help in the experiments performed with the transmission electron microscope.

This work was supported by the Agencia Nacional de Investigación e Innovación (ANII) Uruguay (FCE_1_2019_156706) to JMS. Fellowships from ANII for RI, and “Proyecto de Iniciación” from Comisión Sectorial de Investigación Científica-Universidad de la República del Uruguay. CC is partially supported by FCE_1_2019_156706 and by Programa de Alimentos y Salud Humana (PAyS) IDB - R.O.U. (4950/OC-UR)". AZ is partially supported by Programa de Alimentos y Salud Humana (PAyS) IDB - R.O.U. (4950/OC-UR)"

Authors’ contribution statement

Conceived and designed the experiments: CC, RI, and JMS. Performed the experiments: CC, RI, AZ, and MDP. Analyzed the data: CC, RI, AZ, MDP and JMS. Contributed reagents/materials/analytic tools: MDP and JMS. Wrote the paper: CC, RI, AZ, MDP and JMS. All authors reviewed the results and approved the final version of the manuscript.

Scheme and Figures

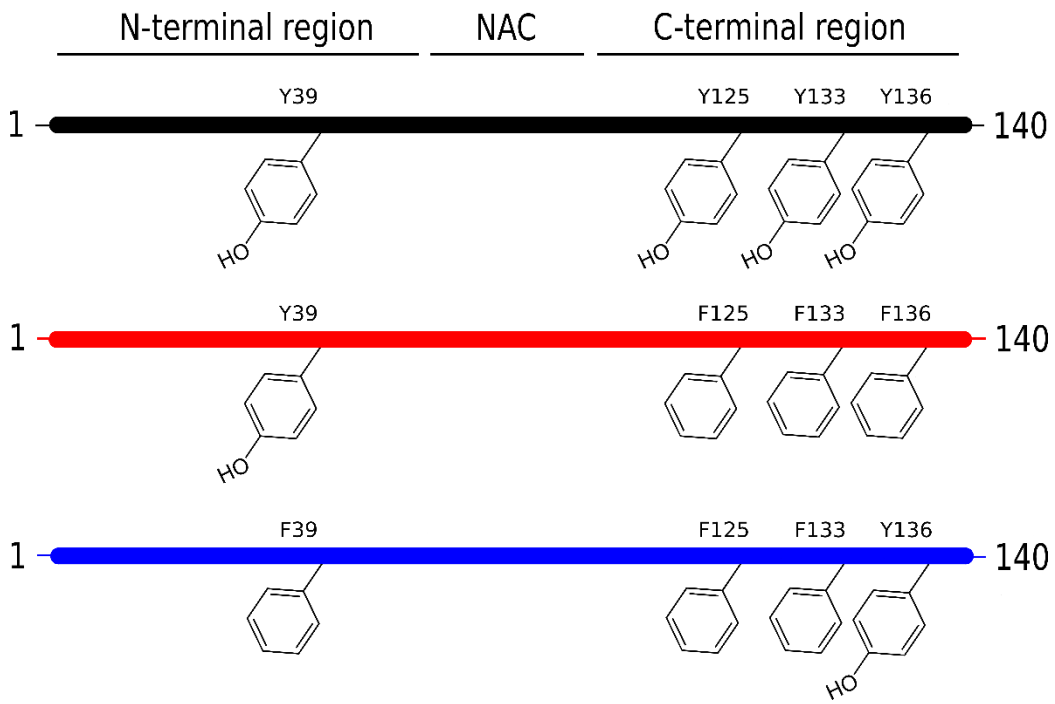

Scheme 1. Scheme illustrating the primary sequence of wild-type a-syn and tyrosine to phenylalanine a-syn mutants. Primary sequence is diagramed indicating the mutated residue. Two mutant forms of a-syn were designed with only one tyrosine residue.

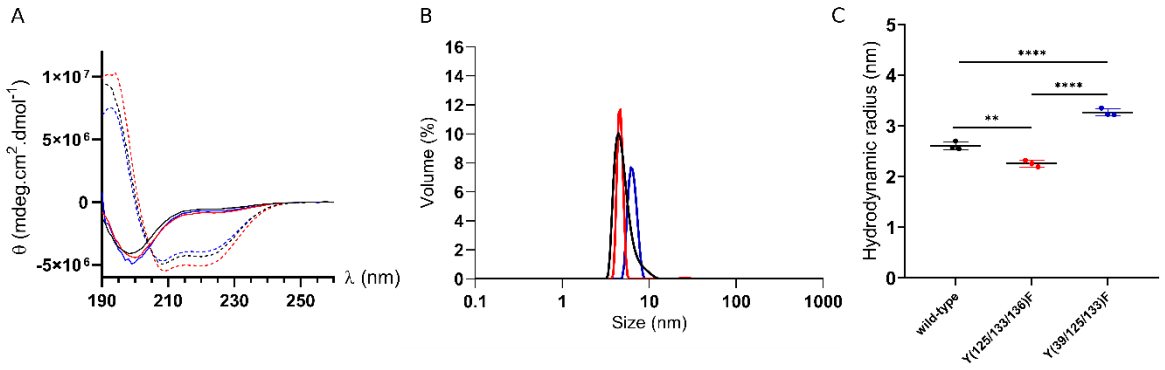

Figure 1. a-Syn mutant constructs characterization for wild-type a-syn (black), mutant Y(125/133/136)F (red), and Y(39/125/133)F (blue). (A) CD spectra obtained for the three proteins in buffer solution (solid line) or with SDS 2 mM (dashed line). (B) Volume percentage as a function of particle size obtained from DLS spectra for monomeric forms of a-syn proteins. (C) Quantification of the hydrodynamic radius obtained for each protein from B. Data are expressed as means of three experiments, ±SD, one-way ANOVA, ** $p < 0.01$, **** $p < 0.0001$.

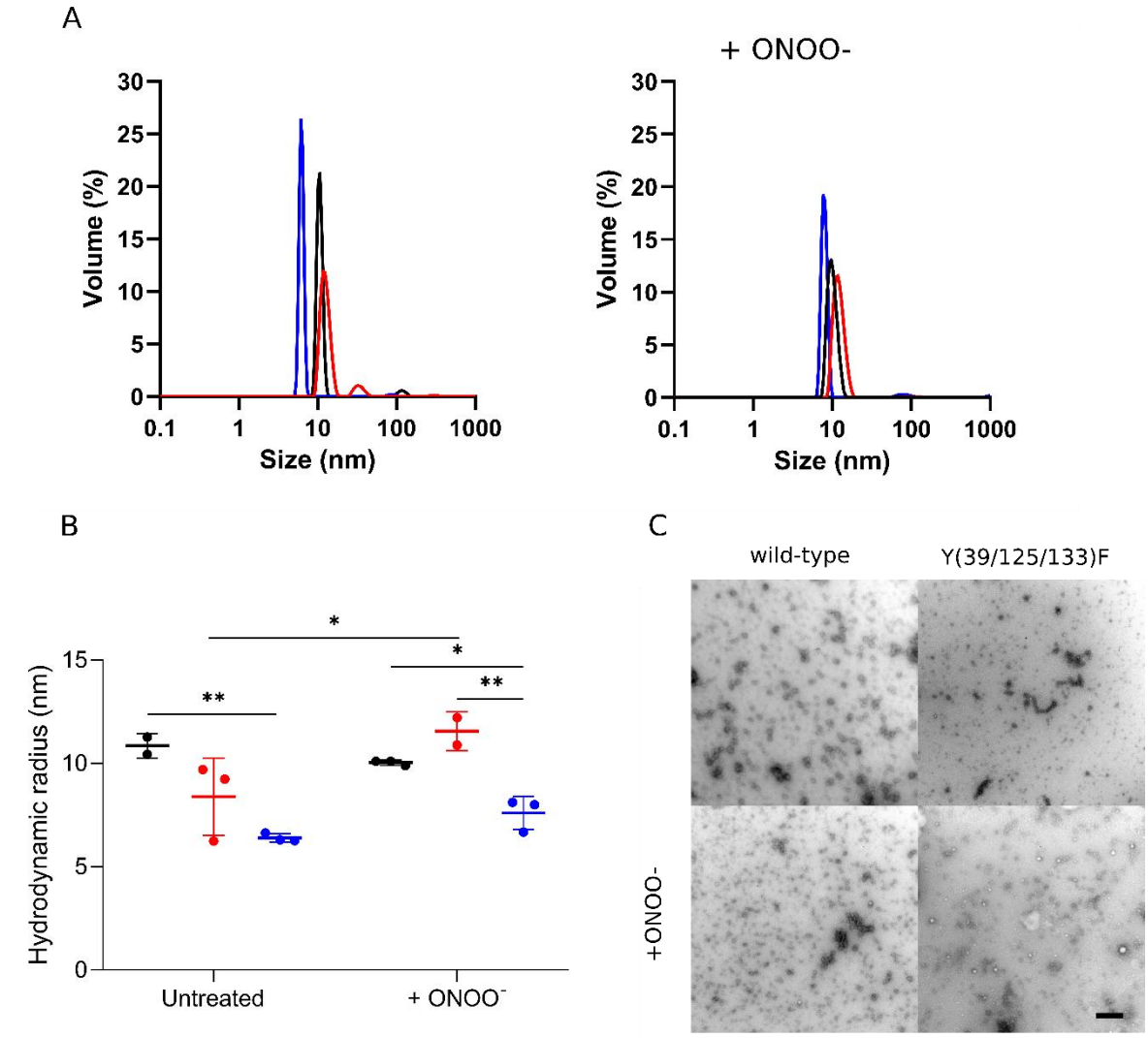

Figure 2. Characterization of a-syn oligomers. (A) Dynamic light scattering showing the volume percentage of oligomers as a function of particle size of wild-type and mutant a-syn and the oligomers generated by wild-type and mutant a-syn treated with peroxynitrite. Wild-type a-syn (black), mutant Y(125/133/136)F (red), and Y(39/125/133)F (blue) (B) Hydrodynamic radius distribution obtained from DLS data (panel A) for oligomeric forms of a-syn proteins (C) TEM images of uranyl acetate stained a-syn oligomer obtained from wild-type a-syn or a-syn mutant Y(39/125/133)F, and the oligomers obtained after treatment with $ONOO^-$. Wild-type a-syn, mutant Y(125/133/136)F, and Y(39/125/133)F. The scale bar corresponds to 500 µm. Data are expressed as means of three experiments, ±SD, two-way ANOVA, * $p < 0.05$, ** $p < 0.01$.

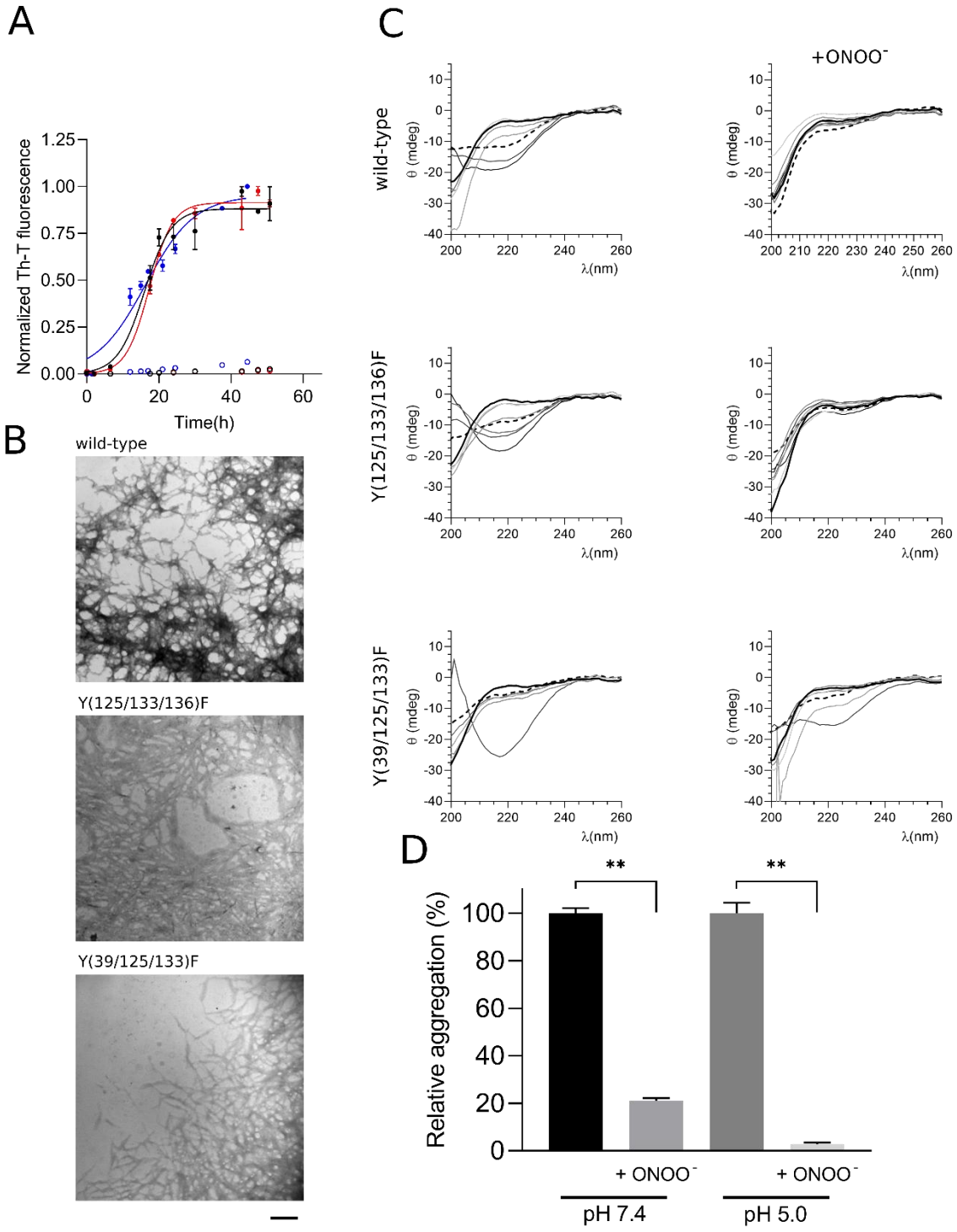

Figure 3. Fibril formation of a-syn proteins was followed by different techniques. (A) Kinetics was measured using Th-T assay for wild-type (black), Y(125/133/136)F (red), and Y(39/125/133)F (blue). a-Syn, untreated proteins (filled circles) or $ONOO^-$ exposed proteins (open circles). (B) End time points of Th-T assay were analyzed by TEM for fibril observation for the untreated proteins. The scale bar corresponds to 500 µm. (C) CD spectra for wild-type a-syn and Y-F mutants. Each grey line corresponds to aliquots

obtained at different time points during protein aggregation assay, before (left) and after (right) the exposure of the protein to the addition of $ONOO^-$. The dotted line corresponds to the aliquot taken at the final aggregation time. (D) Fibril formation of wild-type a-syn was evaluated at different pH and the percentage of inhibition was calculated for the $ONOO^-$ treated protein with respect to untreated controls. Data are expressed as means of three experiments, ±SD. Data are expressed as means of three experiments, ±SD. Unpaired t-test ** $p < 0.01$.

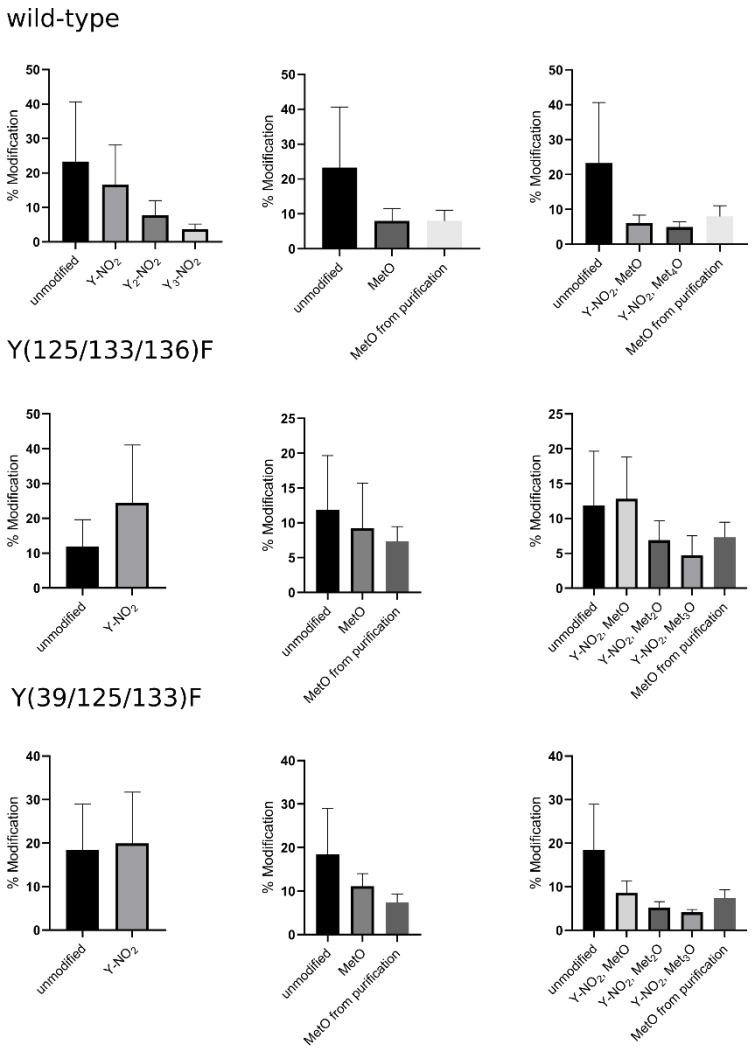

Figure 4. Modification pattern for $ONOO^-$ treated a-syn proteins. The graph at the left represents tyrosine nitration (Y-NO_2). In the middle, methionine oxidation (MetO) and the unmodified protein, MetO from purification corresponds to the basal level of protein oxidation for all samples. At the right, the presence of both oxidative modifications. MS spectra were deconvoluted and compared the peak area for the different species identified as an estimative of the percentage of modification. Data are expressed as means of three experiments, ±SD.

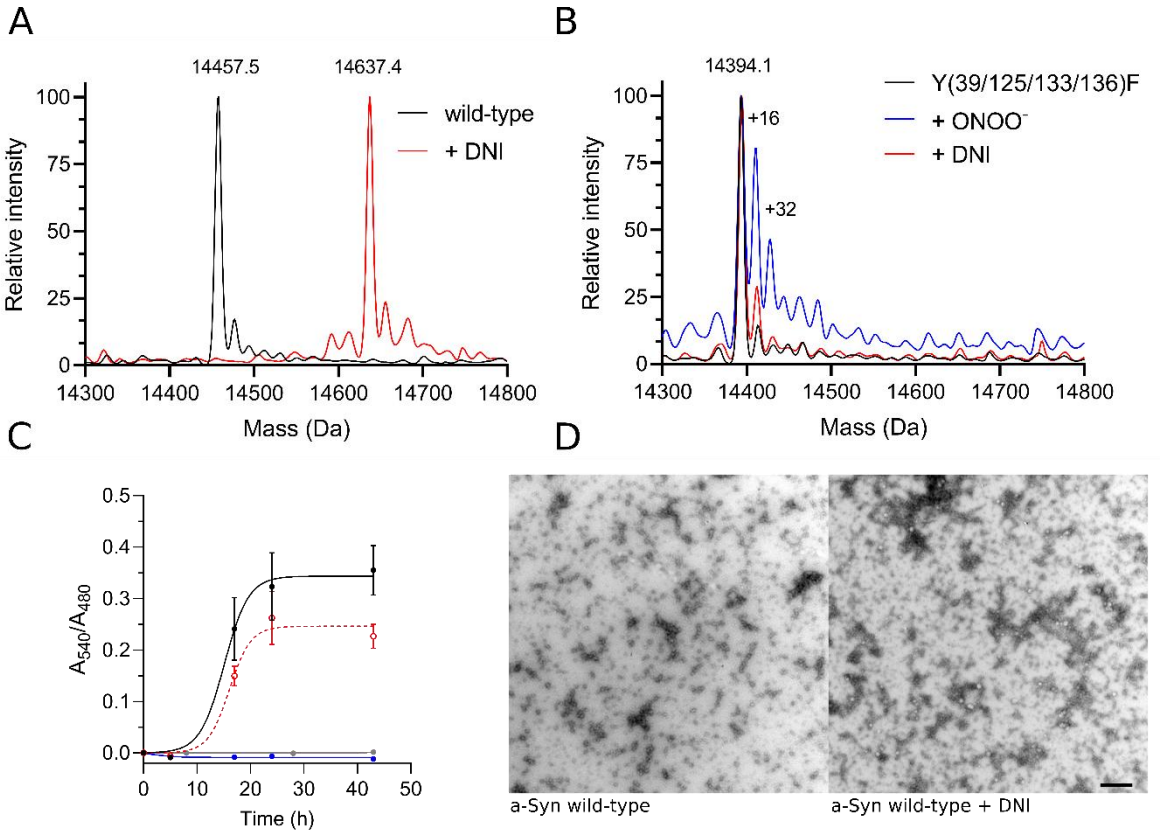

Figure 5. Effect of DNI on nitration of wild-type and mutant Y(39/125/133/136)F a-syn. MS spectra were deconvoluted to show (A) the effect of DNI on wild-type a-syn and in (B) masses of Y(39/125/133/136)F a-syn treated with $ONOO^-$ and DNI. (C) Fibril aggregation measured by Congo Red assay for untreated mutant Y(39/125/133/136)F a-syn (solid black line), Y(39/125/133/136)F a-syn treated with $ONOO^-$ (solid blue line) or DNI (dashed red line), and wild-type a-syn treated with DNI (grey line). (D) TEM images of uranyl acetate stained a-syn wild-type oligomers and nitrated with DNI and UV irradiation (a-syn + DNI). The scale bar corresponds to 500 µm. Data are expressed as means of three experiments, ±SD.

Supplementary information

Supplementary Table 1. Primer sequences

Mutant	Primer	Tm (°C)
a-syn Y39F	Forward 5'-GAGGGTGTTCTC**TTT**GTAGGCTCCAAA-3' Reverse 5'-TTTGGAGCCTAC**AAA**GAGAACACCCTC-3'	62.14
a-syn Y125F	Forward 5'- TCCTGACAATGAGGCT**TTT**GAAATGCCTTCTGAGG-3' Reverse 5'- CCTCAGAAGGCATTTCA**AAA**GCCTCATTGTCAGGA-3'	69.70
a-syn Y133F	Forward 5'-CTGAGGAAGGG**TTT**CAAGACTACGA-3' Reverse 5'-TCGTAGTCTTG**AAA**CCCTTCCTCAG-3'	62.01
a-syn Y136F	Forward 5'-GGTATCAAGAC**TTT**GAACCTGAAGC-3' Reverse 5'-GCTTCAGGTTC**AAA**GTCTTGATACC-3'	60.11
a-syn Y133F/Y136F	Forward 5´-CTGAGGAAGGG**TTT**CAAGAC**TTC**GA-3´ Reverse 5´-TC**GAA**GTCTTG**AAA**CCCTTCCTCAG-3´	62.47

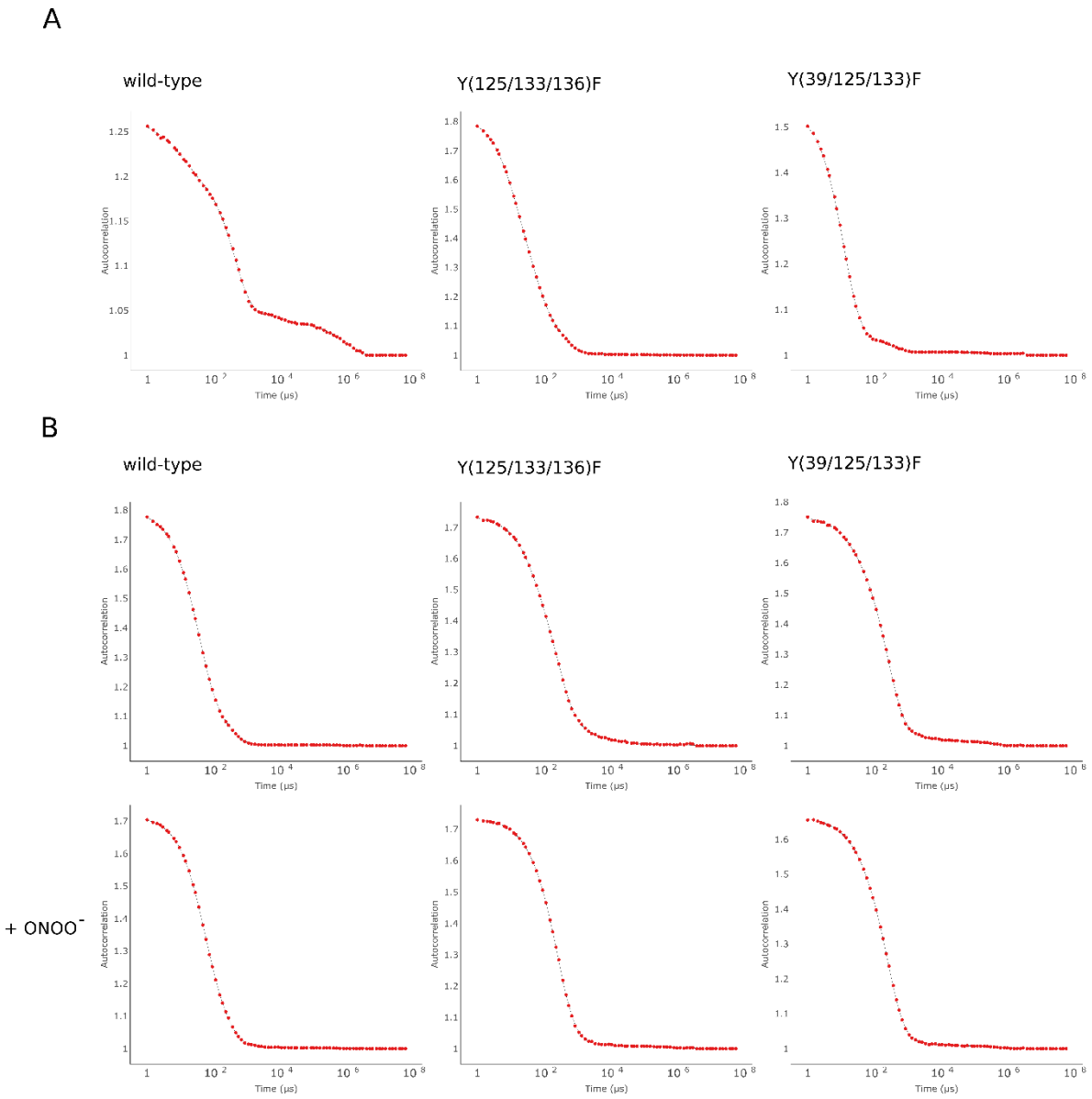

Supplementary Figure S1. Dynamic light scattering data from monomeric and oligomeric a-syn. (A) DLS data and correlation fitting from monomeric wild type, Y(125/133/136)F and Y(39/125/133)F a-syn proteins. (B) DLS data and correlation fitting from the oligomeric wild type, Y(125/133/136)F and Y(39/125/133)F a-syn and the oligomeric species generated from the same proteins treated with $ONOO^-$. The red dots correspond to the DLS data and the black line to the correlation fitting.

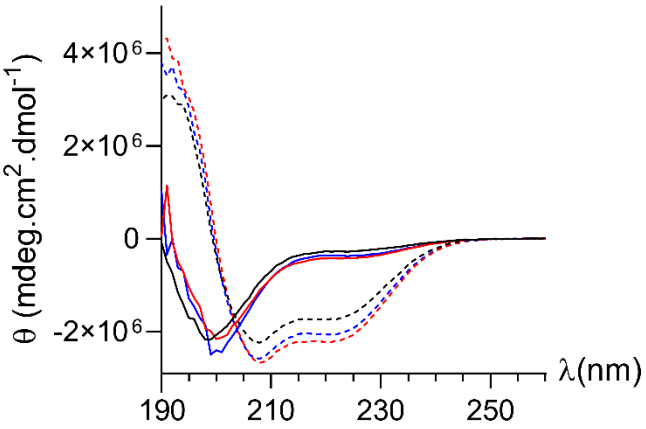

Supplementary Figure S2. Characterization of monomeric proteins after $ONOO^-$ exposure. CD spectra obtained for the three proteins treated with $ONOO^-$ in 20mM phosphate buffer pH 7.4 (solid line) or in SDS 2 mM (dashed line). The different colored lines represent: wild-type a-syn (black) mutant Y(125/133/136)F (red) and mutant Y(39/125/133)F (blue).

References

1. Lee, V. M. Y. & Trojanowski, J. Q. Mechanisms of Parkinson's Disease Linked to Pathological α-Synuclein: New Targets for Drug Discovery. *Neuron* **52**, 33–38 (2006).

2. Burré, J., Sharma, M. & Südhof, T. C. Cell biology and pathophysiology of α-synuclein. *Cold Spring Harb Perspect Med* **8**, 1–28 (2018).

3. Weinreb, P. H., Zhen, W., Poon, A. W., Conway, K. A. & Lansbury Jr., P. T. NACP, a protein implicated in Alzheimer's disease and learning, is natively unfolded. *Biochemistry* **35**, 13709–13715 (1996).

4. Alafuzoff, I. & Hartikainen, P. Alpha-synucleinopathies. in *Handbook of Clinical Neurology* vol. 145 339–353 (Elsevier B.V., 2018).

5. Baba, M. *et al.* Aggregation of alpha-synuclein in Lewy bodies of sporadic Parkinson's disease and dementia with Lewy bodies. *Am J Pathol* **152**, 879–884 (1998).

6. Spillantini, M. G., Crowther, R. A., Jakes, R., Hasegawa, M. & Goedert, M. alpha-Synuclein in filamentous inclusions of Lewy bodies from Parkinson's disease and dementia with lewy bodies. *Proc Natl Acad Sci U S A* **95**, 6469–6473 (1998).

7. Spillantini, M. G. *et al.* Alpha-Synuclein in Lewy bodies. *Nature* **388**, 839–840 (1997).

8. Polymeropoulos, M. H. *et al.* Mutation in the alpha-synuclein gene identified in families with Parkinson's disease. *Science (80-.).* **276**, 2045–2047 (1997).

9. Spillantini, M. G. *et al.* Alpha-synuclein in Lewy bodies. *Nature* **388**, 839–840 (1997).

10. Ghosh, D. *et al.* Structure based aggregation studies reveal the presence of helix-rich intermediate during α-Synuclein aggregation. *Sci. Rep.* **5**, 1–15 (2015).

11. Vidović, M. & Rikalovic, M. G. Alpha-Synuclein Aggregation Pathway in Parkinson's Disease: Current Status and Novel Therapeutic Approaches. *Cells* **11**, 1–31 (2022).

12. Bisi, N. *et al.* α-Synuclein: An All-Inclusive Trip Around its Structure, Influencing Factors and Applied Techniques. *Front. Chem.* **9**, 1–30 (2021).

13. Ferrer-Sueta, G. *et al.* Biochemistry of Peroxynitrite and Protein Tyrosine Nitration. *Chem. Rev.* **118**, 1338–1408 (2018).

14. Hodara, R. *et al.* Functional consequences of alpha-synuclein tyrosine nitration: diminished binding to lipid vesicles and increased fibril formation. *J Biol Chem* **279**, 47746–47753 (2004).

15. Chavarría, C. & Souza, J. M. Oxidation and nitration of alpha-synuclein and their implications in neurodegenerative diseases. *Arch. Biochem. Biophys.* **533**, 25–32 (2013).

16. Souza, J. M., Peluffo, G. & Radi, R. Protein tyrosine nitration-Functional alteration or just a biomarker? *Free Radic. Biol. Med.* **45**, 357–366 (2008).

17. Souza, J. M., Giasson, B. I., Chen, Q., Lee, V. M. Y. & Ischiropoulos, H. Dityrosine cross-linking promotes formation of stable alpha-synuclein polymers. *J Biol Chem* **275**, 18344–18349 (2000).

18. Uversky, V. N. *et al.* Methionine oxidation inhibits fibrillation of human alpha-synuclein in vitro. *FEBS Lett* **517**, 239–244 (2002).

19. Yamin, G., Uversky, V. N. & Fink, A. L. Nitration inhibits fibrillation of human alpha-synuclein in vitro by formation of soluble oligomers. *FEBS Lett* **542**, 147–152 (2003).

20. Giasson, B. I. *et al. Oxidative Damage Linked to Neurodegeneration by Selective alpha-Synuclein Nitration in Synucleinopathy Lesions*. *Science* vol. 290 (2000).

21. Prigione, A. *et al.* Alpha-synuclein nitration and autophagy response are induced in peripheral blood cells from patients with Parkinson disease. *Neurosci. Lett.* **477**, 6–10 (2010).

22. Norris, E. H., Giasson, B. I., Ischiropoulos, H. & Lee, V. M. Effects of oxidative and nitrative challenges on alpha-synuclein fibrillogenesis involve distinct mechanisms of protein modifications. *J Biol Chem* **278**, 27230–27240 (2003).

23. Burai, R., Ait-Bouziad, N., Chiki, A., Lashuel, H. & Lashuel, H. A. Elucidating the role of site-specific nitration of alpha-synuclein in the pathogenesis of Parkinson's disease via protein semisynthesis and mutagenesis. *J. Am. Chem. Soc.* **137**, 5041–5052 (2015).

24. Robinson, K. M. & Beckman, J. S. Synthesis of peroxynitrite from nitrite and hydrogen peroxide. *Methods Enzymol.* **396**, 207–214 (2005).

25. Long, T. *et al.* Light-Controlled Tyrosine Nitration of Proteins. *Angew. Chemie Int. Ed.* **60**, 13414–13422 (2021).

26. Rios, N. *et al.* 5-methyl-1 , 4-dinitro-1 H -imidazole (DNI): synthesis and biochemical characterization. *Free Radic Biol Med* **209**, 116–126 (2023).

27. Apetri, M. M., Maiti, N. C., Zagorski, M. G., Carey, P. R. & Anderson, V. E. Secondary structure of alpha-synuclein oligomers: characterization by raman and atomic force microscopy. *J Mol Biol* **355**, 63–71 (2006).

28. Burastero, O. *et al.* Raynals, an online tool for the analysis of dynamic light scattering. *Acta Cryst.* **79**, 673–683 (2023).

29. Bisaglia, M. *et al.* A topological model of the interaction between α-synuclein

and sodium dodecyl sulfate micelles. *Biochemistry* **44**, 329–339 (2005).

30. Chavarría, C., Rodríguez-bottero, S., Quijano, C., Cassina, P. & Souza, J. M. Impact of monomeric, oligomeric and fibrillar alpha-synuclein on astrocyte reactivity and toxicity to neurons. *Biochem. J.* **475**, 3153–3169 (2018).

31. Chen, S. W. *et al.* Structural characterization of toxic oligomers that are kinetically trapped during α-synuclein fibril formation. *Proc. Natl. Acad. Sci.* **112**, E1994–E2003 (2015).

32. Sokolovsky, M., Riordan, J. F. & Vallee, B. L. Conversion of 3-nitrotyrosine to 3-aminotyrosine in peptides and proteins. *Biochem. Biophys. Res. Commun.* **27**, 21–25 (1967).

33. Bertoncini, C. W. *et al.* Release of long-range tertiary interactions potentiates aggregation of natively unstructured alpha-synuclein. *Proc. Natl. Acad. Sci. U.S.A.* **102**, 1430–1435 (2005).

34. Abello, N., Kerstjens, H. A. M., Postma, D. S. & Bischoff, R. Protein tyrosine nitration: Selectivity, physicochemical and biological consequences, denitration, and proteomics methods for the identification of tyrosine-nitrated proteins. *J. Proteome Res.* **8**, 3222–3238 (2009).

35. Hokenson, M. J. *et al.* Role of individual methionines in the fibrillation of methionine-oxidized alpha-synuclein. *Biochemistry* **43**, 4621–4633 (2004).

36. Karpinar, D. P. *et al.* Pre-fibrillar alpha-synuclein variants with impaired beta-structure increase neurotoxicity in Parkinson's disease models. *Embo J* **28**, 3256–3268 (2009).

37. Winner, B. *et al.* In vivo demonstration that alpha-synuclein oligomers are toxic. *Proc Natl Acad Sci U S A* **108**, 4194–4199 (2011).

38. Volpicelli-Daley, L. A., Luk, K. C. & Lee, V. M. Addition of exogenous alpha-synuclein preformed fibrils to primary neuronal cultures to seed recruitment of endogenous alpha-synuclein to Lewy body and Lewy neurite-like aggregates. *Nat Protoc* **9**, 2135–2146 (2014).

39. Peelaerts, W. *et al.* α-Synuclein strains cause distinct synucleinopathies after local and systemic administration. *Nature* **522**, 340–344 (2015).

40. Cascella, R. *et al.* The release of toxic oligomers from α-synuclein fibrils induces dysfunction in neuronal cells. *Nat. Commun.* **12**, 1–16 (2021).

41. Alam, P., Bousset, L., Melki, R. & Otzen, D. E. A-Synuclein Oligomers and Fibrils: a Spectrum of Species, a Spectrum of Toxicities. *J. Neurochem.* **150**, 522–534 (2019).